251
3-26-81
JWa

(1) Or. 2454

FEBRUARY 1981

PPPL-1754
UC-20f,g

R-3065

MASTER

MODELING OF ICRF HEATING IN PLT

BY

P. L. COLESTOCK, S. L. DAVIS,
J. C. HOSEA, D. Q. HWANG,
H. R. THOMPSON

PLASMA PHYSICS LABORATORY

PRINCETON UNIVERSITY
PRINCETON, NEW JERSEY

This work was supported by the U.S. Department of Energy Contract No. DE-AC02-76-CHO 3073. Reproduction, translation, publication, use and disposal, in whole or in part, by or for the United States government is permitted.

MODELING OF ICRF HEATING IN PLT

P. L. Colestock, S. L. Davis, J. C. Hosea,
D. Q. Hwang, H. R. Thompson

Plasma Physics Laboratory, Princeton University
Princeton, New Jersey 08544 USA

ABSTRACT

Significant heating with the fast magnetosonic wave near the ion cyclotron frequency has been demonstrated in the present generation of tokamaks. Effective wave absorption and heating can be achieved either by using the second harmonic or by heating at the fundamental of a minority ion component. Recent experiments in PLT have facilitated the refinement of a heating model which both shows good agreement with experiment and predicts favorable scaling to hotter, denser plasmas. Details of the model, including full wave theory, power deposition, Fokker-Planck theory, and scaling are discussed.

I. Introduction

In recent years, rf heating research in the ion cyclotron range of frequencies has been focused on the use of the fast magnetosonic wave due to its favorable coupling and penetration properties [1-5]. Much of the work has been directed toward gaining a better understanding of the relevant damping mechanisms in toroidal geometry and has led to the identification of two regimes where effective wave damping and consequent heating are possible: (i) the two-ion regime and (ii) the second harmonic regime. In the two-ion regime the plasma is composed of two ion species with absorption in PLT dominated typically by a minority species at its fundamental cyclotron frequency; bulk ion heating occurs through Coulomb coupling between ion species. For the second harmonic (or higher harmonic) regime, direct bulk ion heating is possible at a weaker rate relative to fundamental heating. In both cases energetic non-thermal ion distributions can be produced whose effective confinement and thermalization is crucial to the overall heating efficiency.

The physics of fast wave heating has been under investigation in the Princeton Large Torus (PLT), both for providing detailed information on the relevant damping mechanism and for testing the scaling of the processes to the multi-megawatt level. Particular emphasis has been placed on identifying heating regimes and coupling configurations which can be readily scaled to a reactor.

Currently, power levels up to 1 MW at 24.6 MHz have been applied to a pair of half-turn loops located on the low field side of the minor cross-section. This frequency is suitable for the two-ion regime with either a hydrogen ($\omega \approx \omega_{ci}$ for B_o = 16 kG), deuterium (32 kG), or ^{3}He (25 kG) minority species. With a separate pair of coils, up to 200 kW at 42 MHz has been used to study pure second harmonic heating in hydrogen (14 kG). These experiments have led to the refinement of a theoretical heating model which shows both good agreement with experiment and a highly favorable prognosis for scaling to hotter, denser plasmas.

In this paper, we describe first the theory of power deposition in the two-ion regime corroborated in part by recent experimental results. The effects of gradients, finite Larmor radius, geometry, and non-Maxwellian ion distributions are discussed in detail. Second, preliminary results in the second harmonic regime are compared with wave damping and particle equilibration calculations. In both regimes, our goal is to develop a self-consistent scaling model for these regimes which can be used to predict the potential for ICRF heating in larger, hotter devices.

II. Two-Ion Regime

The primary function of multiple ion species in the two-ion heating regime is to facilitate wave absorption by inducing a change in polarization at the cyclotron resonance of one or more ion species. Due to screening action in a cold, single-ion plasma under current tokamak conditions, the left-hand (ion) polarized field of the fast wave is suppressed, and consequently, the ion heating is small. However, in a hot plasma, ion Bernstein waves can propagate below the second and higher ion cyclotron harmonics of each species present [6-9]. In locations where the wavelengths of the fast wave and the Bernstein waves are comparable, a rapid change in the wave polarization can occur, giving rise to strong cyclotron damping. In a two-ion plasma the effect takes place between the fundamental frequencies of each species, known as the two-ion hybrid resonance.

The locations where heating takes place occur along vertical layers in the minor cross-section as shown in Fig. 1(a),(b). Two distinct cases can be

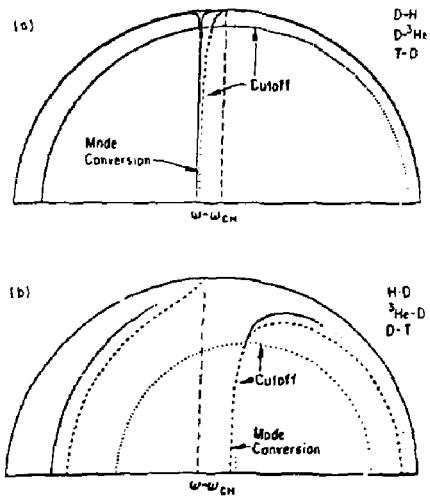

Fig. 1. Wave dispersion surfaces on the plasma cross-section for (a) large e/m ratio minority and (b) small e/m ratio minority.

identified due to the combined effects of density and magnetic field gradients. In Fig. 1(a) is shown the case of a greater e/m ratio minority ion species relative to a lesser e/m majority species. Except for a thin surface region, the fast wave can propagate throughout the plasma. Relative to the excitation source, which is always assumed to be on the low-field side, the waves intercept the minority cyclotron layer before they reach the cutoff-mode-conversion pair. At mode conversion, the Bernstein wave and fast wave can be closely coupled. The case of the minority ion having the lesser e/m ratio is shown in Fig. 1(b). In addition to a reorientation of the cyclotron and mode conversion layers relative to the antenna, a thicker edge evanescent region occurs with possible coupling to the slow wave. This asymmetry of the wave dispersion surfaces signifies an important difference in the wave damping between the two cases and in each situation between incidence from the high and low field sides. A number of workers have attempted to calculate the wave damping using WKB techniques throughout the resonance zone or, assuming low losses, via asymptotic methods [10-13]. Only in the recent work by Swanson [14] has any effort been made to determine the wave damping when the cyclotron layer is close to the cutoff-mode-conversion zone and when the associated losses are high. To this end, we describe a numerical technique to solve for the wave fields in the presence of one-dimensional gradients throughout the resonance zone along with the power deposited in each particle species. The model is applied to minority heating scenarios on PLT and is found to be in substantial agreement with many of the PLT measurements.

Further insight into the nature of the damping process can be gained by an examination of the dispersion relation roots evaluated locally through the resonance zone as shown for typical PLT conditions in Fig. 2. The fast wave

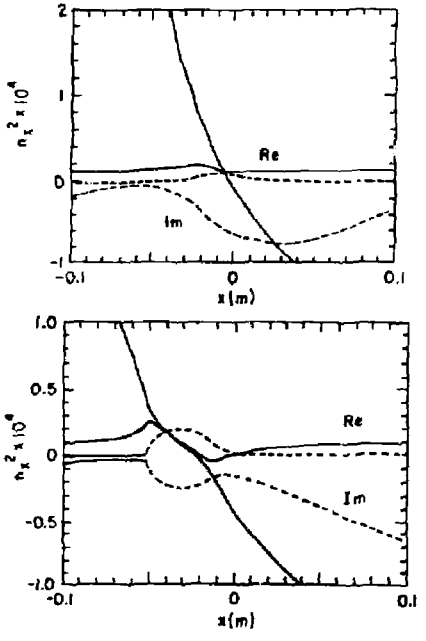

Fig. 2. Dispersion relation roots for (a) weak coupling, $n_H/n_e = 5\%$ and (b) stronger coupling, $n_H/n_e = 30\%$. $n_{eo} = 6 \times 10^{13}$ cm^{-3}, $T_e = 1.2$ keV, $B_T = 17$ kG, $f = 25$ MHz, $k_z = 15$ m^{-1}, $T_D = 1$ keV, $T_H = 0.6$ keV.

propagates from near the plasma edge to the resonance layer, ensuring favorable accessibility from the outside while the ion Bernstein wave facilitates strong wave absorption near the coupling point. In Fig. 2(a) the minority species is sufficiently dilute so that the effect of the Bernstein wave on the fast wave is characterized primarily by an increase in the fast wave absorption. For higher minority concentrations, as shown in Fig. 2(b), a cutoff layer can occur, accompanied by increased reflections for low field incidence and coupling to the Bernstein wave for high field incidence. In either case a theoretical treatment of the problem must include the combined effects of both waves on the total wave absorption.

In order to obtain a quantitative estimate of the wave damping process, we assume the problem may be described by a one-dimensional wave model in the vicinity of the absorption zone. Moreover, we assume that the contributions of the VB particle drifts $-O(r_L/R)$ are small so that the plasma conductivity is given locally by the uniform, hot-plasma conductivity tensor. The latter assumption is justified except in low loss cases where coupling from the fast wave to the Bernstein wave is strong. In such cases the gradient effects serve to reduce the effectiveness of the coupling and must be included. The full wave problem characterized by the dispersion relations of Fig. 2 is a fourth order system which may be integrated numerically with the boundary conditions corresponding to incidence from the low or high field sides. For low field incidence, referring to Fig. 2(a), an incoming wave of unit amplitude is assumed along with the condition that power is only outgoing on the fast and Bernstein wave branches on the high field side. It is also assumed that no power can flow on the cutoff Bernstein branch on the low field side. The solution is obtained by first determining the transfer function across the zone which relates a wave vector on the low field side to one on the high field side. The unknown boundary conditions are rearranged in terms of the known conditions, using the numerically computed transfer functions. The resulting coefficients are then used to regenerate the fields within the zone. For high field incidence, the roles of the incoming and outgoing wave on the fast wave branch are reversed. Typical results for the dilute minority case are shown in Fig. 3. The cases of low field incidence [Fig. 3(a)] and high field incidence [Fig. 3(b)] are shown for the dispersion relation roots depicted in Fig. 2(a). For high field incidence the Poynting flux decreases by 60% in traversing the absorption zone while a small amount of the power, ~10%, appears in the short wavelength Bernstein wave branch. In the case of low field incidence, the absorbed power is nearly the same, but somewhat less coupling to the Bernstein wave from the low field side is predicted. In either case, reflections from the layer are negligible (<2%). The power partitioning among species can be determined from the expression

$$\left.\frac{\partial S_x}{\partial x}\right|_\sigma = \frac{\varepsilon_0 \omega}{4}\, \underline{E}^* \cdot \underline{\underline{K}}^a_\sigma \cdot \underline{E}$$

where $\underline{\underline{K}}^a$ is the anti-Hermitian part of the dielectric tensor and σ denotes the contribution from the σth species. The results for the above case are shown in Fig. 4(a) and 4(b) for low and high field incidence, respectively. It is noted that even for this weak coupling case, a strong asymmetry in the power absorption develops. For low field incidence the power is absorbed primarily by the minority (H) species while for incidence from the high field side, roughly equal amounts of majority (D) and minority heating are predicted. The asymmetry in the damping suggests that the Bernstein wave plays a key role

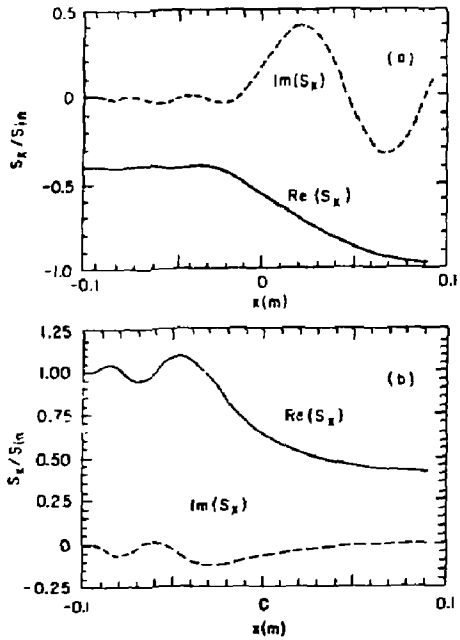

Fig. 3. (a) Poynting flux for a wave incident from the low field side for the weak coupling case in Fig. 2(a), $P_{ref} = 2.8\%$, $P_{trans} = 40.0\%$, $P_{abs} = 57.1\%$, (b) high field incidence for the same case, $P_{ref} = 0.02\%$, $P_{trans} = 40.6\%$, $P_{mode\ converted} = 1.8\%$, $P_{abs} = 57.1\%$.

in determining the nature and extent of the damping, even in the weakly coupled case. As such, the absorption must be calculated using the full wave solution, including the localized Bernstein wave fields. It is found that for sufficiently weak coupling, the solution approaches that obtained by WKB methods and recovers symmetry with respect to direction of incidence. It is also of interest to note that the oscillations on the high field side are a result of the juxtaposition of the fast and Bernstein waves but do not represent negative energy. Rather, these oscillations imply an exchange of energy from electromagnetic (or electrostatic) to kinetic which is possible because of the finite temperature of the plasma. The total energy, electromagnetic plus kinetic, is found to be constant apart from dissipative losses. As such, the integral under the Poynting flux, over a sufficiently wide region so that the oscillations have damped away, represents the total power lost. In the case of stronger coupling, achieved by raising the minority concentration, the asymmetry between low and high field incidence widens because of the possibility of reflections from the cutoff on the low field side and strong mode conversion from the high field side (Fig. 5). Even with increased reflections, minority heating dominates from the low field side since both incident and reflected waves traverse the minority cyclotron layer. The consequence of this fact is that minority heating can be expected to dominate even when the minority species concentration is an appreciable fraction of the majority concentration.

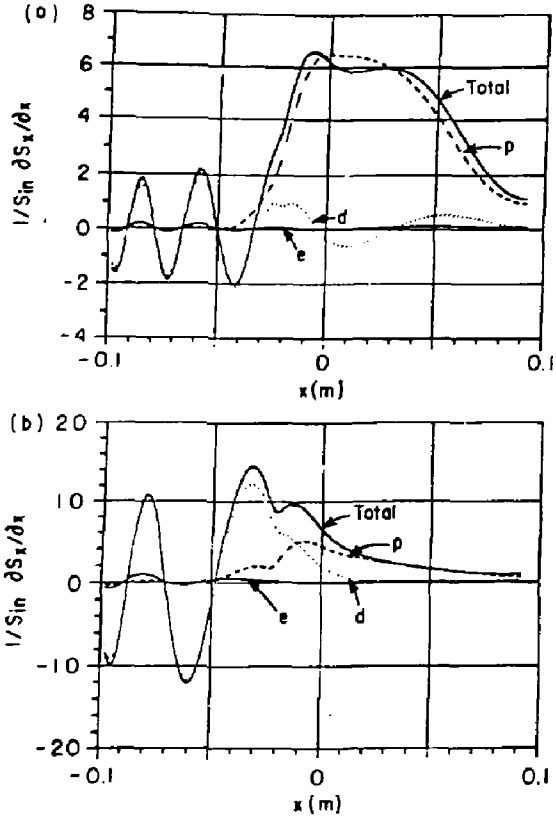

Fig. 4. Derivative of the Poynting flux for (a) low field incidence and (b) high field incidence for the weak coupling case in Fig. 2(a). Total absorbed power is equal to the sum of the changes in Poynting and kinetic fluxes across the layer.

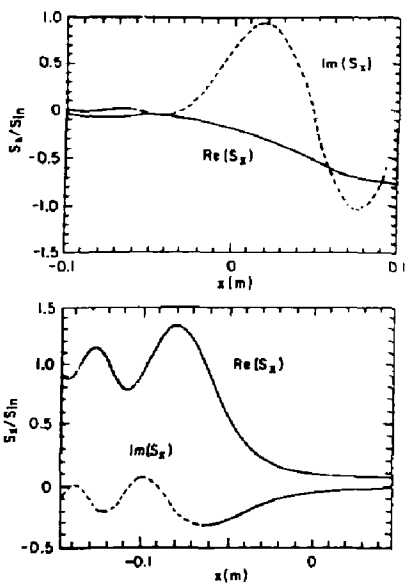

Fig. 5. (a) Poynting flux for a wave incident from the low field side for stronger coupling case in Fig. 2(b), $P_{ref} = 27.4\%$, $P_{trans} = 5.8\%$, $P_{mode\ converted} = 0.8\%$, $P_{abs} = 66.9\%$. (b) high field incidence $P_{ref} = 0.07\%$, $P_{mode\ converted} = 23.2\%$, $P_{abs} = 70.9\%$.

An important consideration which must be taken into account in these calculations is the two-dimensional character of the source and plasma. While an exact solution of the wave fields in this case is cumbersome, an estimate of the two-dimensional effects can be made using geometric optics techniques. The field at a point just outside the absorption zone is calculated as a superposition of all rays which subtend the finite-sized antenna. The amplitude transport along each ray is determined, including first order refractive effects which treat the wave energy density as a fluid conserved within each ray bundle. The process gives good agreement with numerically calculated eigenmodes in the presence of radial density gradients (Fig. 6) even when the radial wavelength is comparable to the density scale length.

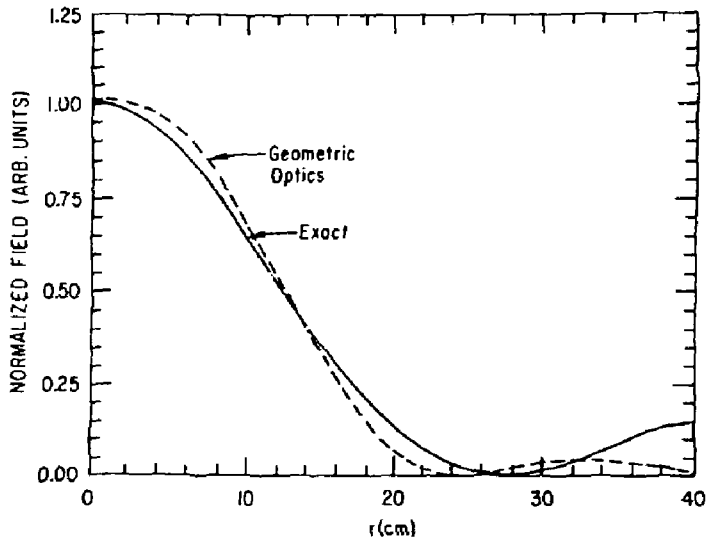

Fig. 6. Comparison of the exact numerical solution of the fast wave eigenfunction with a parabolic radial density profile and the fields constructed by geometric optics techniques.

A further complication results when non-Maxwellian ion distributions are taken into account. Stix has shown theoretically [15], and it has been observed experimentally [16], that energetic ion distributions are generated as a consequence of rf-induced velocity diffusion for particles transiting the resonance layer. Once created, the presence of a hot ion species tends to further enhance the damping rate until the hot species, typically, can be responsible for nearly all the wave absorption. In order to estimate this effect, an isotropic Fokker-Planck code [17] is solved numerically to determine the ion distribution using an initial guess for the radial power deposition profile. Since the resulting distribution function monotonically decreases with energy, it can be represented by a group of Maxwellian distributions of decreasing density and increasing temperature. A new power deposition profile is obtained by averaging the plane wave calculations described above over a magnetic surface. The process is iterated and is found to

converge quickly, resulting typically in a substantial enhancement of the hot ion absorption.

The above theoretical model can be applied to relevant large e/m minority heating scenarios in PLT [18], namely D-H and D-^{3}He, and the results for typical parameters are shown in Fig. 7. Both cases show a strongly centrally peaked power deposition profile with the D-^{3}He case slightly more peaked due to the combined effects of differences in the wave dispersion and ion distribution temperatures. Based on these profiles, ion power balance [19] calculations have been carried out which show good agreement with experimental profiles (Fig. 8). In the D-H case a substantial amount of the power flows to the electrons through Coulomb coupling to the minority species while virtually all the minority power goes to the ions in the D-^{3}He case. Moreover, a significant amount of power can be lost by H charge exchange in the D-H case which does not occur in the D-^{3}He case. In either case, the minority species accounts for nearly all the applied power giving rise to high efficiency bulk plasma heating, provided the energetic ions are well confined.

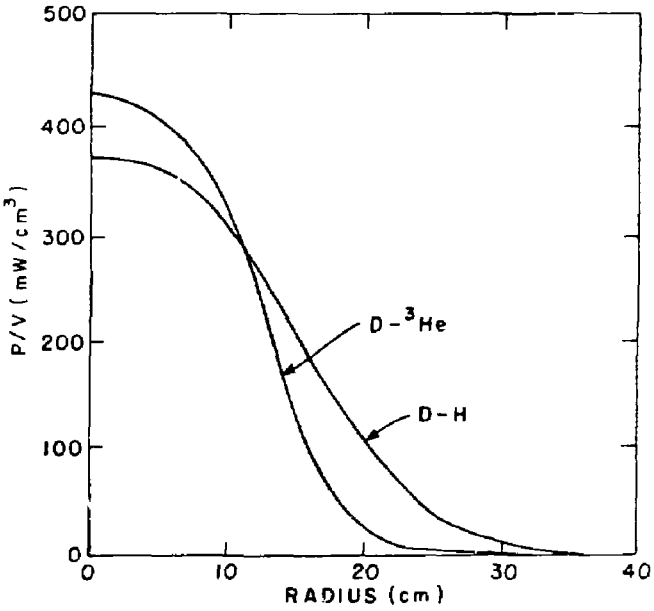

Fig. 7. Calculated power deposition profiles for the D-H and D-^{3}He cases with 350 kW rf power, $n_{e0} = 3 \times 10^{13}$ cm^{-3}, 10% = n_{min}/n_e.

Further support for the absorption model described above can be obtained from low e/m minority heating measurements. In this situation the cyclotron layer occurs on the high field side of the cutoff and can be effectively shielded from low field excitation at sufficiently high minority concentration. This shielding effect can be observed as a sudden onset of neutron production in the case of an H-D plasma when the deuterium concentration is varied from 5 to 10 percent (Fig. 9) [20]. For the parameters

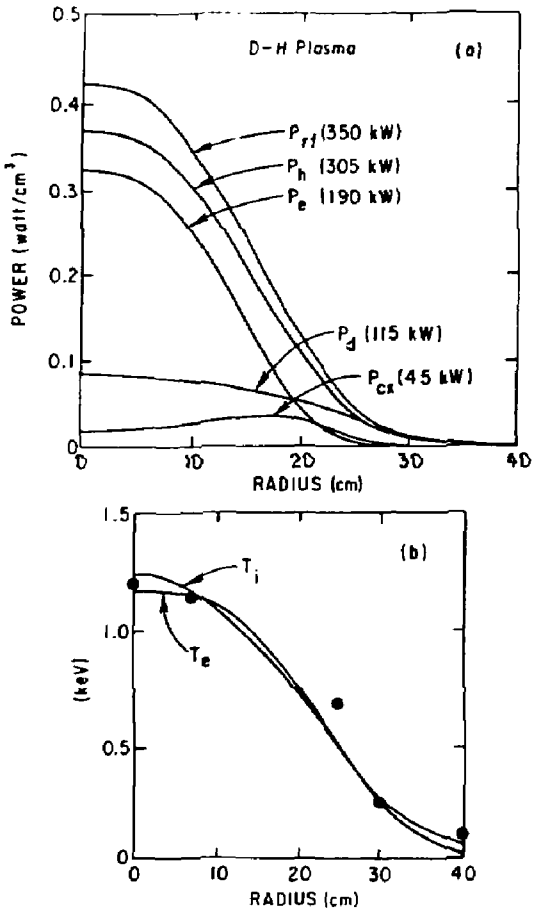

Fig. 8. (a) Calculated ion power balance profiles for the D-H case with 350 kW rf power based on experimental electron temperature and density profiles. (b) Calculated ion temperatures with experimental ion temperature points determined by charge exchange and spectroscopy measurements.

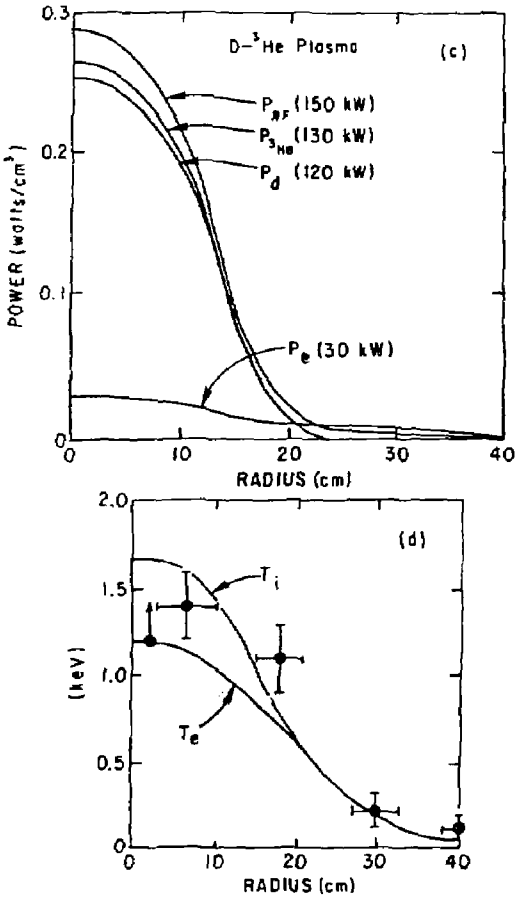

Fig. 8. (c) Calculated profiles for the D-^{3}He case with 150 kW rf power. (d) Calculated ion temperature profiles with experimental points.

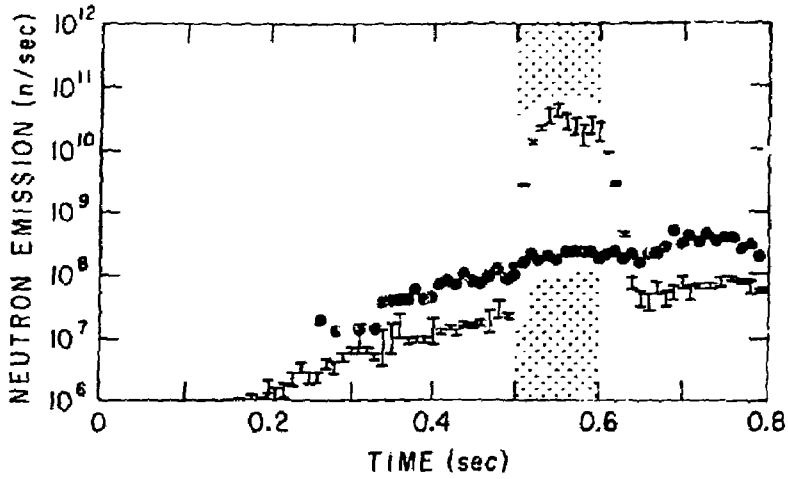

Fig. 9. Neutron production from an H-D plasma. $\bar{n}_e \sim 5 \times 10^{13}$ cm^{-3}, $P_{rf} \sim 450$ kW. (I) Deuterium minority concentration of 5% and (●) 10%. Electron density has been kept constant.

shown here the single pass absorption decreases from 30% at a 5% D level to 3% at a 10% D level while the reflection coefficient from the cutoff layer increases from 20% to 60%. The neutron production in this case is observed to decrease with increasing density. According to the Fokker-Planck theory, the deuterium tail energy should decrease with increasing density. This inverse dependence in the H-D case may be due to the appearance of a thick evanescent zone and possible coupling to the slow wave in the surface as shown in Fig. 1(b). Another possible contributing factor was the fact that n_D/n_H decreases with increasing n_e since n_D was held fixed in these experiments. As such, the single-pass damping on the deuterons is predicted to increase rapidly as n_D/n_H decreases. Similar measurements were made in a ^{3}He plasma with a deuterium minority and the opposite dependence (D energy decreasing with increasing n_e) was found. In this situation the edge evanescent layer is comparatively thin, and the slow wave does not propagate in the surface near the antenna. Moreover, the n_D/n_H ratio where the mode conversion (cutoff) is expected to onset occurs at a higher value than that of the H-D case. Thus direct deuteron damping can occur throughout the density range studied. It is also of interest to note that when a deuterium tail is produced in the ^{3}He-D case that significant electron heating is also observed (Fig. 10). This heating can be accounted for in part by coupling from the minority ions and partly by tight coupling with the bulk ions.

Of some theoretical interest is the case when the ion species have comparable concentrations. In this situation the two-ion cutoff-mode conversion zone is rather opaque ($\lesssim$20% transmission) and relatively lossless due to the

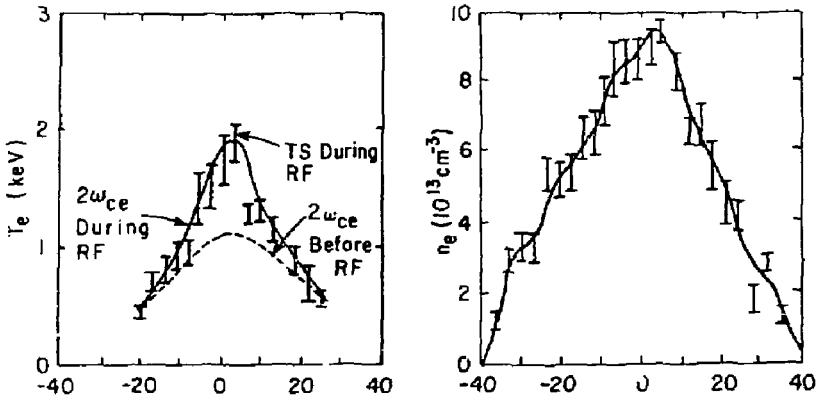

Fig. 10. Electron heating in a D-^{3}He plasma. P_{rf} ~ 600 kW. Electron temperature measurements via $2\omega_{ce}$ cyclotron emission and Thomson scattering. Both diagnostics agreed both before and during rf pulse.

large separation from the resonance layers. From the high field side mode conversion is strong, and the resulting ion Bernstein wave damping can give rise to both low e/m ion and electron heating. This result is in rough agreement with previously reported heating in the TFR device where excitation is primarily from the high field side. From the low field side, reflection is nearly complete (≥80%) and should result in standing waves between the reflecting layer and the wall. This is, however, not the case observed on PLT. High e/m species (H) heating dominates when either the cutoff-mode-conversion layer or the hydrogen resonance is placed on axis. A possible explanation for this heating is the fraction of power which, by tunneling and reflection, can approach the mode conversion layer from the high field side. Other effects which may play a role in broadening the cyclotron resonance include shear, finite amplitude fields, and the effects of gradients which have all been neglected here. For the case of strong reflections for low field incidence, it may also be necessary to carefully determine the full two-dimensional mode structure in order to determine accurately the amount of power which, by multiple reflections, can reach the mode conversion from the high field side. Nonetheless, large e/m heating in the 50/50 case remains largely unexplained with the present model.

III. Second Harmonic Regime

The theoretical model described in the previous section is readily applied to second or higher harmonic heating as well. The effect of the Bernstein wave on the fast wave polarization is similar to that described for the two-ion regime; however, the range over which mode conversion can occur is narrower and the overall heating rate is somewhat weaker. Nevertheless, the change in polarization produces a significant enhancement of the damping at the second harmonic over that expected from a consideration of finite Larmor radius effects alone.

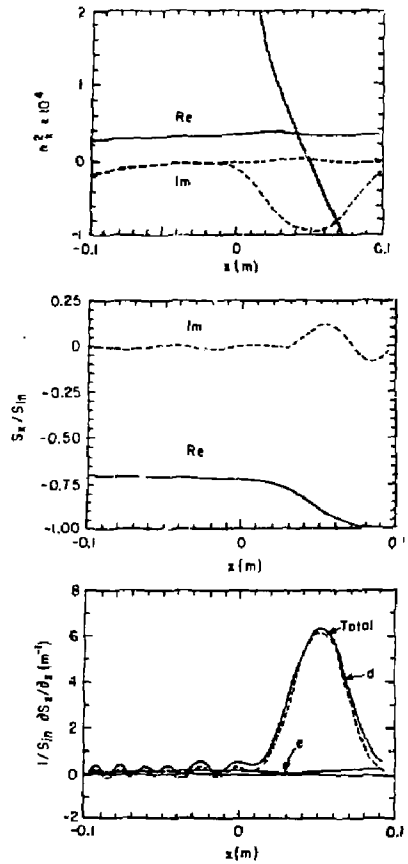

Fig. 11. (a) Dispersion relation roots for second harmonic case in PLT. $n_{eo} = 6 \times 10^{13}$ cm^{-3}, $B_t = 14.3$ kG, $f = 42$ MHz, $k_z = 13$ m^{-1}, $T_D = 0.6$ keV, $T_e = 1.2$ keV. (b) Poynting flux for low field incidence, $P_{ref} = 0.2\%$, $P_{trans} = 70.4\%$, $P_{abs} = 29.5\%$, (c) derivative of Poynting flux.

The dispersion relation roots along with the expected absorption for typical PLT parameters are shown in Fig. 11. The Bernstein wave is only weakly coupled to the fast wave but produces single-pass damping of ~30% which is ample to suppress toroidal eigenmode formation. The resulting loading is characterized by a high overall background level (Fig. 12) and does not require mode tracking for optimization of coupling. The resultant heating efficiency is found to be comparable to that observed in the two-ion regime.

Of particular importance is the fact that the second harmonic driven ion distribution is stable and does not run away in time. This result can be predicted from a Fokker-Planck theory which includes the full rf diffusion operator, including the effects of finite Larmor radius. The inclusion of FLR terms has the effect of reducing the diffusion at high energies. A fully nonlinear Fokker-Planck code, including self-ion collisions, has been used to model the second harmonic heating case shown above, and the results for the isotropic case are shown in Fig. 13. The overall tail energy and time

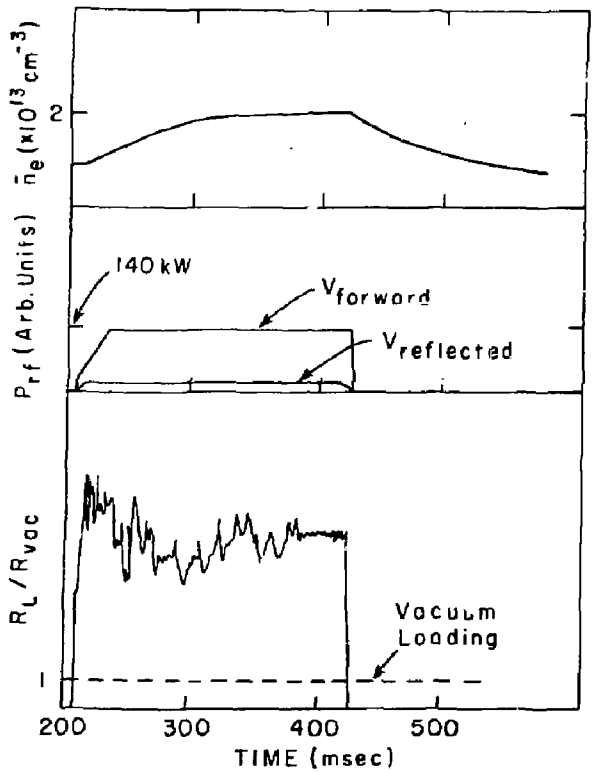

Fig. 12. Time evolution of density, forward and reversed power, and derived loading for second harmonic case.

evolution agree with experiment when a sharply peaked power deposition profile ≤5 cm is assumed. This assumption is roughly consistent with the narrow deposition profile calculated from the full wave theory.

IV. Summary and Discussion of Scaling

It is clear from the above discussion that minority heating is an efficient means to heat plasma in present day tokamak with sufficiently good fast ion confinement. Depending on the energy of the rf-induced minority ion tail, both bulk electrons and ions can be heated with comparable efficiencies and in a manner similar to the slowing down of neutral beams. The primary mechanism for wave damping arises from the favorable finite Larmor radius effect of an ion Bernstein wave on the fast wave polarization. As such, the absorption is expected to increase with increasing density and temperature.

A number of promising possibilities for efficiently coupling to the fast wave are evident from these experimental results. Coupling from the low field side is feasible and attractive from the reactor point of view. Coil loading is expected to remain high at higher densities, and the damping of eigenmodes

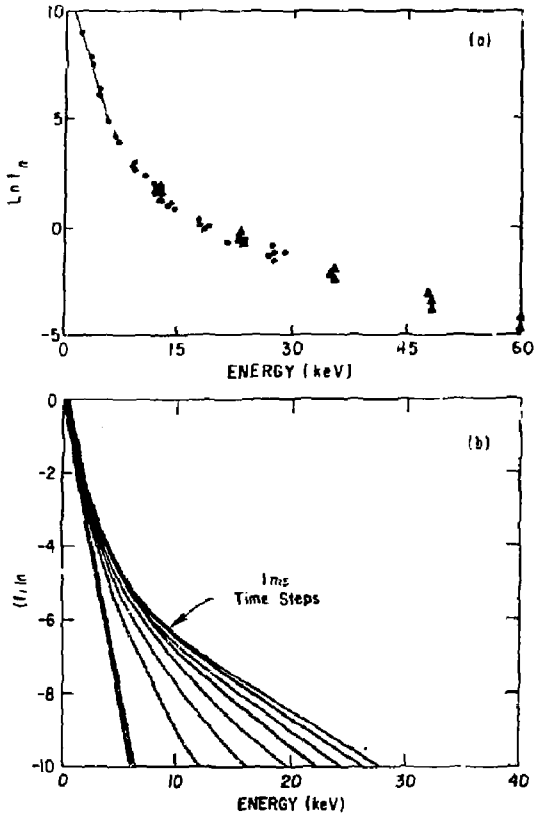

Fig. 13. (a) Majority hydrogen charge exchange distribution for the case of Fig. 12. (b) Calculated hydrogen distributions via Fokker-Planck theory in 1 ms time steps from rf turn-on to saturation.

precludes the necessity of mode tracking in order to optimize the coupling. Moreover, at the higher frequencies possible with second and higher harmonic heating, waveguide excitation is feasible which could greatly simplify the materials requirements of the coupling system in a reactor.

Several ion heating scenarios also emerge from these results as possible candidates for heating in reactors. Minority heating of hydrogen in a D-T plasma allows the possibility of waveguide coupling (≥65 MHz) from the low field side. Minority ^{3}He heating in deuterium affords the interesting possibility of a driven D-^{3}He device although fundamental ^{3}He heating will most likely require loop excitation. Second harmonic ^{3}He, deuterium, and even hydrogen (as a minority species) appear to be feasible and attractive because of the fortunate combination of strong absorption with the possibility of waveguide coupling. Based on the scaling model discussed herein, third harmonic (deuterium) heating should also be possible in a reactor, roughly equivalent to the second harmonic absorption rate for present PLT conditions.

The use of the fast wave to heat reactor plasma appears to be feasible. Coupling and wave penetration at high density is good and scales approximately according to linear theory up to the 1 MW/antenna levels tested thus far in PLT. Efficient ion heating has been observed and has been shown to be crucially dependent on the fast ion confinement which, in current and future devices, is adequate. Experiments are currently underway in PLT to further explore the scaling and heating physics to the multimegawatt level.

Acknowledgements

The authors wish to acknowledge discussions with F. W. Perkins, T. H. Stix, and G. Swanson and the continuing support of Drs. H. P. Furth and M. B. Gottlieb. The authors are also indebted to J. Q. Lawson and J. M. Perron and their staffs for expert technical assistance and to the PLT research staff for their diagnostic support. This work was supported by U. S. Department of Energy Contract No. DE-AC02-76-CH03073.

References

[1] ADAM, J., SAMAIN, A., Association Euratom - C.E.A. Report EUR-CEA-FC-579 (Fontenay-aux-Roses, 1971); ADAM, J., Report EUR-CEA-FC-711 (Fontenay-aux-Roses, 1973).

[2] ADAM, J. AND ST GROUP, Proceedings 5th International Conference on Plasma Physics and Controlled Nuclear Fusion Research (Tokyo, 1975), Vol. I. IAEA, Vienna, 65.

[3] HOSEA, J. C., *Princeton University Report PPPL-1309 (1976).*

[4] EQUIPE TFR, Proceedings 3rd International Meeting on Theoretical and Experimental Aspects of Heating of Toroidal Plasmas (Grenoble, 1976), Vol. I. Centre D'Etudes Nucleaires de Grenoble, 87.

[5] VDOVIN, V. L., SHAPOTKOVSKII, N. V., ROSANOV, V. D., Proceedings 3rd International Meeting on Theoretical and Experimental Aspects of Heating of Toroidal Plasmas (Grenoble, 1976), Vol. II. Centre D'Etudes Nucleaires de Grenoble, 349.

[6] WEYNANTS, R. R., Phys. Rev. Lett. 33 (1974) 2.

[7] SWANSON, D. G., NGAN, Y. C., Phys. Rev. Lett. 35 (1975) 8.

[8] SWANSON, D. G., Phys. Rev. Lett. 36 (1976) 6.

[9] JACQUINOT, J., MCVEY, B. D., SCHARER, J. E., Phys. Rev. Lett. 39 (1977) 2.

[10] NGAN, Y. C., SWANSON, D. G., Phys. Fluids 20 (1977) 11.

[11] PERKINS, F. W., Nucl. Fusion 17 (1977) 1197.

[12] JACQUINOT, J., Proceedings 3rd Topical Conference on RF Plasma Heating (Pasadena, 1978), Paper D4; JACQUINOT, J., Proceedings Joint Varenna-Grenoble International Symposium on Heating in Toroidal Plasmas (Grenoble, 1978), Vol. I. Centre D'Etudes Nucleaires de Grenoble, 127.

[13] SCHARER, J. E., MCVEY, B. D., MAU, T. K., Nucl. Fusion 17 (1977) 2.

[14] SWANSON, D. G., Phys. Fluids 21 (1978) 6.

[15] STIX, T. H., Nucl. Fusion 15 (1975) 737.

[16] HOSEA, J. C., et al., Phys. Rev. Lett. 43 (1979) 1802.

[17] HOSEA, J. C., et al., in Course and Workshop on Physics of Plasmas Close to Thermonuclear Conditions, Varenna, Italy, August 1979.

[18] HWANG, D. Q., et al. in Joint Conference of 4th Kiev International Conference on Plasma Theory and 4th International Congress on Waves and Instabilities in Plasmas (Nagoya, Japan) April 7-11, 1980.

[19] BRUSATI, M., DAVIS, S. L., HOSEA, J. C., STRACHAN, J. D., SUCKEWER, S., Nucl. Fusion 18 (1978) 1205.

[20] HOSEA, J. C., et al., in 8th International Conference on Plasma Physics and Controlled Nuclear Fusion Research (Brussels, Belgium, 1980) IAEA-CN-38/D-5-1.